

# Microslip friction in flat belt drives

L Kong and R G Parker\*

Department of Mechanical Engineering, Ohio State University, Columbus, Ohio, USA

*The manuscript was received on 31 March 2005 and was accepted after revision for publication on 14 July 2005.*

DOI: 10.1243/095440605X31959

**Abstract:** The microslip shear model of belt mechanics is extended to fully incorporate belt inertia effects and used to analyse the steady state of a two-pulley drive. The belt is modelled as an axially moving string consisting of a tension-bearing member and a pliable elastomer envelope. Relative displacement between the tension-bearing member and the pulley surfaces shears the elastomer envelope, transferring the friction from the pulley surface to the tension-bearing member. The belt–pulley contact arcs consist of adhesion and sliding zones. Static friction exists in the adhesion zones, whereas kinetic friction exists in the sliding zones. An iteration method involving one outer and two inner loops is proposed to find the steady mechanics, including the sliding and adhesion zones, belt–pulley friction, and belt tension distribution. The outer loop iterates on the tight span tension similar to that used in published creep models. Two inner loops iterate on the tight span and driven pulley speeds respectively, necessitated by the speed differences between the tension-bearing member and the pulley at the entry points in the shear theory. Comparisons between the shear and creep models are conducted. Dramatic differences in belt–pulley mechanics between these two models are highlighted. Nevertheless, the key system performance measures such as the belt tight/slack span tensions, the maximum transmissible moment, and efficiency differ only modestly for the most normal operating conditions. Correspondingly, the adoption of the creep model for flat belts in industry is well justified because it is well developed and simple, although the shear model seems more relevant for modern belts with grid layers.

**Keywords:** belt drives, microslip layer, shear friction, pulley–belt interaction

## 1 INTRODUCTION

Belt drives are widely used to transmit power or motion in industry. Belt mechanics normally refers to the study of the steady state interaction between belt and pulleys including friction, belt tension, and speed and so on [1]. Important system performance criteria such as belt slip and power efficiency result from such analyses. Generally, power efficiency is a paramount concern in power transmission applications, whereas belt slip is of more concern in motion transmission applications. Two kinds of belt slips exist in belt drives: global and partial (or micro) slips. Global belt slip means full slip along the entire contact arc such that the belt has nearly

rigid body motion relative to the pulley; this should be avoided in all applications. Partial belt slip, unavoidable in most cases as the resulting friction is needed to transmit the power, reduces system performance, especially for precision motion transmission applications such as in data tape recorders. Partial belt slip makes the pulley rotation transmission ratio different from the nominal one, resulting in transmission error (a similar concept exists in gear mechanics).

One of the key studies in belt mechanics is to describe the friction interaction between the belt and pulleys. No generally accepted friction model exists in the literature. Furthermore, discrepancies in friction behaviour exist between theoretical prediction and practically observed behaviours, as communicated by belt drive manufacturers. Two different theories, both physically motivated but based on different belt–pulley friction assumptions, are developed in the literature.

\*Corresponding author: Department of Mechanical Engineering, Ohio State University, 650 Ackerman Road, Columbus, OH 43202, USA.

The first theory is the creep model, which assumes that the existence of friction depends completely on the relative motion (creep) between the belt and the pulley surfaces [1]. Only kinetic friction is considered in the belt–pulley interaction. The belt either slides (creeps) on the pulley surfaces or completely adheres to the pulley surfaces having constant tension and the same speed as the pulley in the adhesion zone. It results that the belt–pulley contact arc is divided into two different zones [2]: an adhesion zone and a sliding zone. Only the sliding zone contributes to moment transmission through friction forces, whereas the friction remains zero in the adhesion zone. This model, developed by Euler [3], is well known and widely adopted in industrial applications. Comprehensive review of this work can be found in references [4, 5]. Recent incorporation of factors such as belt inertia [6, 7], bending stiffness [8, 9], and pulley grooves [10, 11] has made this model more mature. Most of the analyses are applied to two-pulley drives.

The second theory is the shear model, which was first proposed by Firbank [12]. It assumes that the belt consists of a pliable elastomer or a rubber envelope (to grip the pulley surfaces) and a strong tension-bearing member, usually from high modulus cords (see the belt cross-section in Fig. 1(a)). The bottom of the pliable elastomer envelope adheres to the pulley surface if the friction force is zero or less than the maximum static friction force. Otherwise, it slides over the pulley surfaces resulting in kinetic friction force. The friction force in the adhesion zone is determined by the shear deformation, i.e. the relative tangential motion between the pulley surfaces and the tension-bearing member. Although Firbank states that the shear model addresses mainly very stiff belts that can be viewed as inextensible, belt extensibility can still be incorporated into this model (fig. 6 in reference [12]). It is not belt extensibility but rather the different friction assumptions concerning the pliable elastomer layer that distinguish the shear model from the well-established creep model. In fact, belt extensibility is of most importance for the complete solution of the entire belt drive including the free spans, through which the solutions on different pulleys are coupled with each other.

The shear model was developed three decades ago and its study is still limited to a single driver or driven pulley, although more factors such as belt extensibility and belt radial compliance have been considered [1, 10]. No analysis of this shear model on a complete practical belt drive has been conducted. Correspondingly, no system criteria such as power efficiency or the maximum transmissible moment have been investigated, using this model. This greatly limits its application. In this study, the shear model is applied to a two-pulley drive, the most common application

in an industry, and an iteration method is proposed to find the complete system's steady state mechanics. Although the analysis is for flat belts, poly-ribbed belts, widely used in automotive and other industries, can be reasonably approximated as flat belts. Belt inertia is incorporated into the traditional shear model to improve the modelling accuracy; it has been neglected in prior research. The iteration method proposed here can be naturally extended to a multi-pulley drive.

This shear microslip model can be used in applications other than belt drives. For example, by assuming an idealized elasto-plastic shear layer of negligible thickness between two friction surfaces, Menq *et al.* [13] propose a similar microslip model and successfully use it to explain the significant reduction of the resonant response in frictionally damped structures. Although Menq *et al.* proposed their model independently for a different purpose without reference to Firbank [12], these two models share many similarities and the foundation ideas are the same. Both are physically motivated by the observation that the elastic materials transmitting friction experience shear deformation in their contact surfaces, resulting in microslip.

## 2 GOVERNING EQUATIONS OF A BELT OVER PULLEY SURFACES

Figure 1(a) shows a two-pulley belt drive where the driver and driven pulleys have the same radius,  $R$ . The subscripts 1 and 2 represent the driver and driven pulleys, respectively;  $\varphi_i$  ( $i = 1, 2$ ) is the angle measured from the belt entry points on the pulleys. The belt tensions in the tight and slack spans are  $F_t$  and  $F_s$ , respectively. From the continuity condition,  $F_t$  equals the belt tension at the entry point on the driver pulley  $F_1(0)$ , whereas while  $F_s$  equals that on the driven pulley  $F_2(0)$ , where the pulley quantities are the functions of  $\varphi_1$  and  $\varphi_2$ . Similar continuity conditions exist for the belt speed, i.e.  $V_t = V_1(0)$  and  $V_s = V_2(0)$ .

The belt consists of two components: the stiff tension-bearing member, usually cords, and the wrapping elastomer envelope. The elastomer envelope functions as a shear layer between the tension-bearing member and the pulley surfaces. Because of the motion of the tension-bearing member relative to the pulley surfaces, shear deformation and stress develop in this elastomer layer to transmit the friction force to the tension-bearing member. This shear layer behaves as an ideal elasto-plastic material: when the friction force is less than the maximum static friction, the bottom of the shear layer sticks to the pulley surfaces; otherwise, it slides over the pulley surface resulting in kinetic

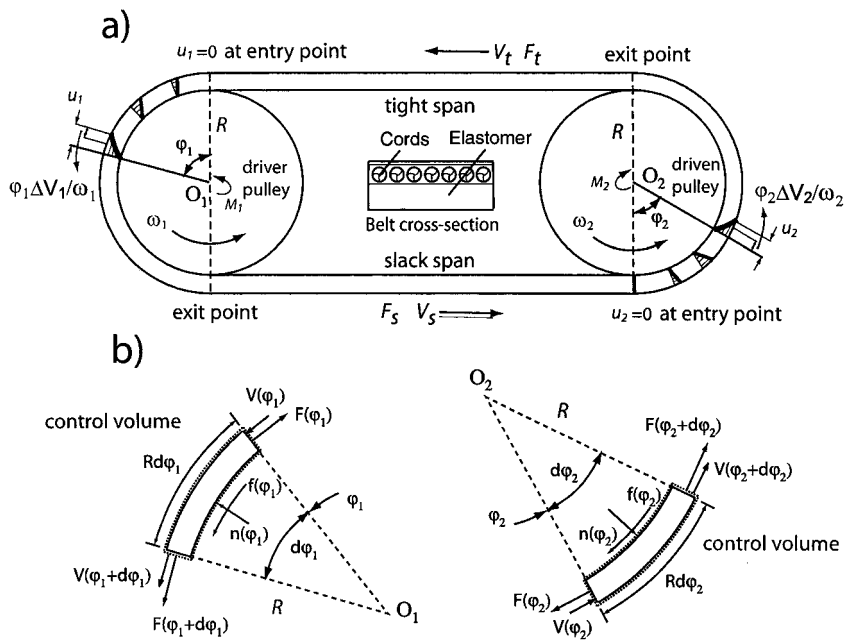


**Fig. 1** (a) A two-pulley belt drive. (b) Free body diagrams of the belt on the driver and driven pulleys

friction. This contrasts with the creep theory where no friction force exists in the adhesion zones.

Figure 1(b) shows the free body diagrams of the belt (in the control volume) on the driver and driven pulleys. Belt inertia is fully considered.  $G = mV$  is the constant mass flowrate, where  $m$  is belt mass density per unit length and  $V$  the belt average speed over the cross-section. In this study, the belt (average) speed  $V$  is approximated by the speed of the tension-bearing member (the speed of the elastomeric layer varies in the cross-section from the shear deformation, although the speed variation is very small). Balance of linear momentum projected in the tangential and normal directions yields

$$\frac{d(F_i - GV_i)}{Rd\phi_i} = f_i \quad \frac{(F_i - GV_i)}{R} = n_i \quad i = 1, 2 \quad (1)$$

where  $f_i$  and  $n_i$  are contact forces per unit arclength exerted on the belt.

A constitutive law relating belt tension  $F$  and velocity  $V$  completes the problem [6–9, 14]. Then the constitutive law is

$$F = EA \left( \frac{m_0 V}{G} - 1 \right) \quad (2)$$

where  $EA$  is the belt longitudinal stiffness and  $m_0$  is the belt mass density per unit length in the stress-free state, which can be measured.

At the belt entry points, it is assumed that the elastomeric envelope contact point sticks to the pulley surfaces and there is no shear in the elastomer [1]. For the belt at an arbitrary point  $\phi_i$ , the tangential displacement of the tension-bearing member relative to the pulley surface comes from two components. The first one,  $(\phi_i/\omega_i)\Delta V_i$ , is due to the speed difference between the belt and the pulley at the entry point, where  $\Delta V_i = V_i(0) - R\omega_i$ . The second component  $\int_0^{\phi_i} [\varepsilon(\phi_i) - \varepsilon(0)]Rd\phi_i$  is from the extensibility of the belt, where  $\varepsilon(\phi_i) = F_i(\phi_i)/EA$  is the belt strain and  $\varepsilon(0) = F_i(0)/EA$  is the belt strain at the entry point. Summation of these two components leads to the total shear deflection along the pulley tangent

$$u_i = \frac{\phi_i}{\omega_i} \Delta V_i + \int_0^{\phi_i} [\varepsilon(\phi_1) - \varepsilon(0)]Rd\phi_i \quad i = 1, 2 \quad (3)$$

If the bottom of the elastomer layer adheres to the pulley surface, the friction force produced in the shearing layer is

$$f_i = ku_i \quad i = 1, 2 \quad (4)$$

where the shear stiffness  $k = \tilde{G}B/H$ ,  $\tilde{G}$  is the belt shear modulus,  $B$  the belt width, and  $H$  the belt height [1].

Equations (3) and (4) hold when the friction force is less than the maximum static friction, i.e.  $ku_i \leq \mu_s n_i$ , where  $\mu_s$  is the static friction coefficient. When the shear deflection  $u_i > \mu_s n_i/k$ , the belt slides on the pulley surfaces, leading to a sliding zone.

Substitution of equations (3) and (4) into equation (1) yields the governing equation in the adhesion zone

$$\frac{d(F_i - GV_i)}{R d\varphi_i} = f_i = k \left[ \frac{V_i(0) - R\omega_i}{\omega_i} \varphi_i + \int_0^{\varphi_i} \frac{F_i - F_i(0)}{EA} R d\varphi_i \right] \quad i = 1, 2 \quad (5)$$

Differentiation of equation (5) with respect to  $\varphi_i$  yields

$$\frac{d^2(F_i - GV_i)}{d\varphi_i^2} = \frac{kR^2}{EA} [F_i - F_i(0)] + kR \frac{V_i(0) - R\omega_i}{\omega_i} \quad i = 1, 2 \quad (6)$$

Use of the constitutive law (2) leads to an expression for the tractive tension  $T = F - GV$

$$V = \frac{G}{m_0} \left( 1 + \frac{F}{EA} \right) \Rightarrow T = F - GV = \left( 1 - \frac{G^2}{m_0 EA} \right) F - \frac{G^2}{m_0} \quad (7)$$

Substitution of the first set of equation (7) into equation (6) yields

$$\left( 1 - \frac{G^2}{m_0 EA} \right) \frac{d^2 F_i}{d\varphi_i^2} = \frac{kR^2}{EA} [F_i - F_i(0)] + kR \frac{V_i(0) - R\omega_i}{\omega_i} \quad i = 1, 2 \quad (8)$$

which can be further rewritten as

$$\frac{d^2 F_i}{d\varphi_i^2} - N^2 F_i = -N^2 \left[ F_i(0) - EA \frac{V_i(0) - R\omega_i}{R\omega_i} \right], \quad N^2 = \frac{(kR^2/EA)}{1 - (G^2/m_0 EA)} \quad i = 1, 2 \quad (9)$$

The general solution of equation (9) is

$$F_i = F_i(0) - EA \frac{V_i(0) - R\omega_i}{R\omega_i} + C_1 e^{N\varphi_i} + C_2 e^{-N\varphi_i} \quad i = 1, 2 \quad (10)$$

where  $C_1$  and  $C_2$  are constants to be determined from the boundary conditions. At the beginning of the adhesion zone (entry point), the belt tension is  $F_i(0)$ , giving

$$C_1 + C_2 = EA \frac{V_i(0) - R\omega_i}{R\omega_i} \quad (11)$$

There is no shear at the entry point, i.e.  $[dF_i/d\varphi_i]_{\varphi_i=0} = 0$ , which leads to  $C_1 = C_2$ . Thus, the belt tension in the adhesion zone is

$$F_i = F_i(0) + EA \frac{V_i(0) - R\omega_i}{R\omega_i} [\cosh(N\varphi_i) - 1] \quad i = 1, 2 \quad (12)$$

Substitution of equation (12) into equation (5) gives the friction force in the adhesion zone

$$f_i = \left( \frac{V_i(0) - R\omega_i}{R\omega_i} \right) \left( \frac{k}{N} \right) \sinh(N\varphi_i) \quad i = 1, 2 \quad (13)$$

In the sliding zones, the belt governing equation is the same as that for the sliding zones in the creep model [7]

$$\frac{d(F_i - GV_i)}{R d\varphi_i} = f_i = \mu_k \frac{F_i - GV_i}{R} \quad i = 1, 2 \quad (14)$$

where  $\mu_k$  is the kinetic friction coefficient. The belt tension and speed vary exponentially with respect to the angular coordinate  $\varphi_i$ , as can be solved from equation (14) and the constitutive law (2) [7].

Different from the creep model where the belt tension and speed are constant and there is no friction in the adhesion zone, moment can be transmitted in the adhesion zone for the shear model because of the static friction force. If the moment to be transmitted is small, it is possible that there is only an adhesion zone (no sliding zone) in each of the belt-pulley contact arcs. In such cases, the maximum friction force occurs at the belt exit points, and its value is less than or equal to the maximum static friction.

In the cases where both adhesion and sliding zones exist, the transition point occurs where the friction force equals the maximum static friction. For example, for the driver pulley

$$k \left[ \int_0^{\alpha_1} \frac{F_1 - F_t}{EA} R d\varphi_1 + \frac{V_1(0) - R\omega_1}{\omega_1} \alpha_1 \right] = -\mu_s \frac{F_1(\alpha_1) - GV_1(\alpha_1)}{R} \quad (15)$$

where the transition angle  $\alpha_1$  is less than the belt wrap angle on the driver pulley. The belt wrap angles on the pulleys can be calculated from the drive geometry based on contact points on lines of common tangency between the pulleys (because belt bending stiffness is not considered here [8]). For drives where the driver and driven pulleys have the same radius, the wrap angles on both pulleys

are  $180^\circ$ . Substitution of equation (13) into equation (15) leads to

$$\left[ \frac{V_1(0) - R\omega_i}{\omega_1} \right] \left[ \frac{\sinh(N\alpha_1)}{N} \right] \left( \frac{kR}{\mu_s} \right) + \left( 1 - \frac{G^2}{m_0EA} \right) \left\{ F_t + EA \frac{V_1(0) - R\omega_i}{R\omega_1} [\cosh(N\alpha_1) - 1] \right\} - \frac{G^2}{m_0} = 0 \quad (16)$$

A similar equation can be found for the transition point  $\alpha_2$  delimiting the adhesion and sliding zones on the driven pulley.

### 3 SOLUTION FOR A TWO-PULLEY BELT DRIVE

The steady motion analysis is presented for a two-pulley belt drive where the driver and driven pulleys have the same radius and friction coefficients. However, the present method extends naturally to a general belt drive with different pulleys. The specified parameters are driver and driven pulley radius  $R$ , centre distance  $L$  between the two fixed pulleys, belt longitudinal stiffness  $EA$ , rotation speed  $\omega_1$  of the driver pulley, static and kinetic friction coefficients  $\mu_s$  and  $\mu_k$ , belt mass density per unit length  $m_0$  in the stress-free state, total unstretched belt length  $L^{(0)}$ , and the moment  $M_2$  transmitted to the driven pulley. For flat belt drives, because there is no moment loss [6–8], the moment on the driver pulley is always the same as that on the driven pulley, i.e.  $M_1 = M_2$ . These two moments are called the driving moment  $M$  in the following analysis.

A prominent distinction of the shear model compared with the creep model is that the belt and pulley speeds are not the same at the entry points. This feature complicates the solution procedure and necessitates two additional iteration loops to find the speed differences at these points, in contrast with the one iteration loop for the creep model [8].

The iteration method involves three loops: one outer and two inner ones. The solution flowchart is depicted in Fig. 2 and discussed subsequently.

#### 3.1 Two inner loops for an assumed tight span tension

Supposing the tight span tension is known (or assumed in an iteration process as indicated in the top box of Fig. 2), then the steady state of the belt on the driver pulley can be calculated first. This requires iteration on the tight span speed  $V_t$ . For any assumed value of  $V_t$ , the mass flow rate  $G$  is obtained from the constitutive law (2). For the

symmetric drive, the problem is defined over the range  $0 \leq \varphi_1 \leq 180^\circ$ . The steady state of the belt tension, speed, and friction is solvable, using the equations derived in the previous section, for the case of a single pulley. From this, the moment from the friction  $\tilde{M}_1$  can be calculated and checked against the known moment  $M_1$ . The tight span speed is adjusted and this iteration process continues until the correct belt speed (for the assumed tight span tension) is found. This is the belt speed that makes the moment from the friction equal to  $M_1$ , the specified driving moment to be transmitted.

After the steady state of the belt on the driver pulley is obtained, the second inner iteration loop finds the driven pulley rotation speed. Different from the driver pulley, the belt speed and tension at both the entry and exit points are known; it is the rotation speed of the driven pulley that is unknown and needs to be determined in this loop. Similar to the previous iteration loop on the tight span speed, the iteration of the driven pulley rotation speed  $\omega_2$  stops when the moment calculated from the friction force  $\tilde{M}_2$  equals the specified driving moment  $M_2$ .

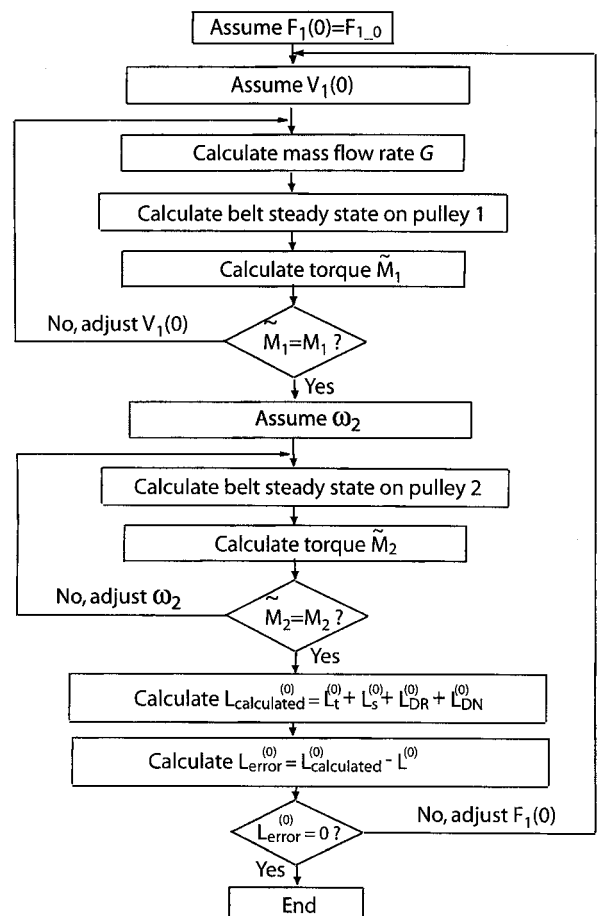


Fig. 2 Flowchart of the three-loop iteration method to find the steady state drive mechanics

### 3.2 Outer loop for the tight span tension

In the earlier mentioned two inner iteration loops, it is assumed that the tight span tension is known. However, in the analysis, the tight span tension is not known *a priori*. Determination of this value needs a criterion or a compatibility condition. The compatibility condition is from the physical requirement that the unstretched belt length back calculated from the steady state must equal the user-specified stress-free belt length  $L^{(0)}$  [7, 8]. Mathematically, this is

$$\sum_{i=1}^2 (L_{\beta_i}^{(0)} + L_{\alpha_i}^{(0)}) + L_t^{(0)} + L_s^{(0)} = L^{(0)} \quad (17)$$

where  $L_{\beta_i}^{(0)}$  and  $L_{\alpha_i}^{(0)}$  are unstretched lengths of the sliding and adhesion zones ( $\alpha_i$  is the adhesion angle and  $\beta_i$  is the sliding angle), and  $L_t^{(0)} = L/(1 + F_t/EA)$  and  $L_s^{(0)} = L/(1 + F_s/EA)$  are the unstretched lengths of the tight and slack spans, respectively.  $L_{\beta_i}^{(0)}$  and  $L_{\alpha_i}^{(0)}$  are readily available from the belt steady motion calculated in the previous inner loops. The tight span tension is adjusted in the outer loop (with the two inner loops repeated accordingly) and the process repeats until convergence of equation (17) is achieved within a chosen tolerance.

## 4 RESULTS AND DISCUSSION

Results are presented for a two-pulley drive where the physical properties are listed in Table 1. The moments on the driver and driven pulleys are equal and vary together in this study. Results from the creep model are also presented, and the difference between the shear and creep models is highlighted (see reference [8] for details of the creep model and the solution method).

Figure 3 shows the variation of the adhesion and sliding angles with the driving moment for the shear and creep models. The differences between these two models are apparent. For the shear model, there are three different stages (Fig. 3(a)) as the driving moment increases. When the driving moment is small ( $M < 1.2$  N m), only adhesion zones exist on both the driver and the driven pulleys. When the driving moment is in the middle range ( $1.2$  N m  $< M < 2.5$  N m), the driver pulley develops a sliding zone in addition to the adhesion zone,

**Table 1** Physical properties of the example belt drive with two identical pulleys

$R_1 = R_2 = 0.05$ m	$L = 0.1571$ m	$EA = 25$ kN
$\mu_k = 0.6$	$\mu_s = 0.72$	$m_0 = 0.0056$ kg/m
$\omega_1 = 500$ r/min	$L^{(0)} = 0.6271$ m	$k = 9000$ kN

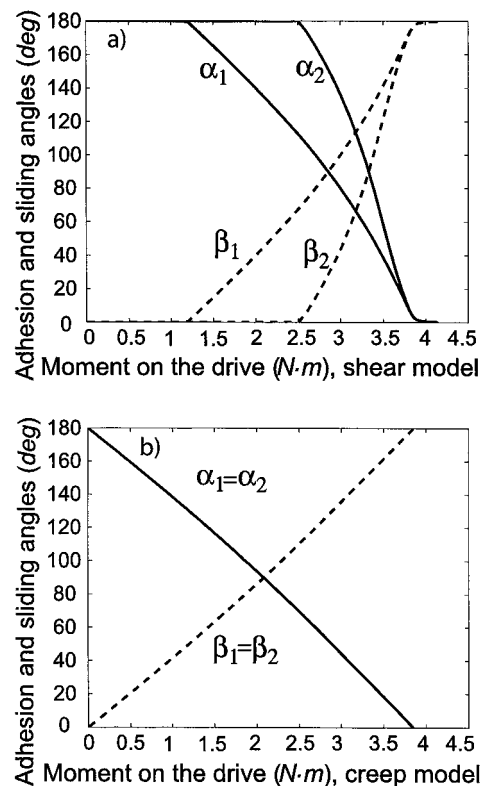


**Fig. 3** Variation of the adhesion and sliding angles on the driver and the driven pulleys for the system specified in Table 1: (a) shear model and (b) creep model

whereas the driven pulley remains with only an adhesion zone. Finally, for large driving moments ( $M > 2.5$  N m), each pulley has both sliding and adhesion zones. In contrast, for the creep model, no matter how small the driving moment is, sliding zones always exist on both pulleys because only the sliding zones contribute to transmission of the moment [8]. For the symmetric example drive with  $R_1 = R_2 = R$ , the adhesion and sliding zones on the driver and driven pulleys are always the same for the creep model (Fig. 3(b)). This symmetry is broken for the shear model (Fig. 3(a)).

The distinctly different friction force distributions on the driver and driven pulleys for both models are shown in Figs 4 and 5. Both models have friction force discontinuities at the transition points separating adhesion and sliding zones (Fig. 3). However, the variations of belt tension on the driver and driven pulleys are continuous but with discontinuous slope for the creep model and smoothly varying for the shear model (Figs 6 and 7). For both models, the difference between the tension (solid lines) and the tractive tension (dashed lines),  $GV$ , varies little over the range. This indicates that the belt speed  $V$  changes little in the drive because  $G$  is constant. This can also be seen from the constitutive law (2),

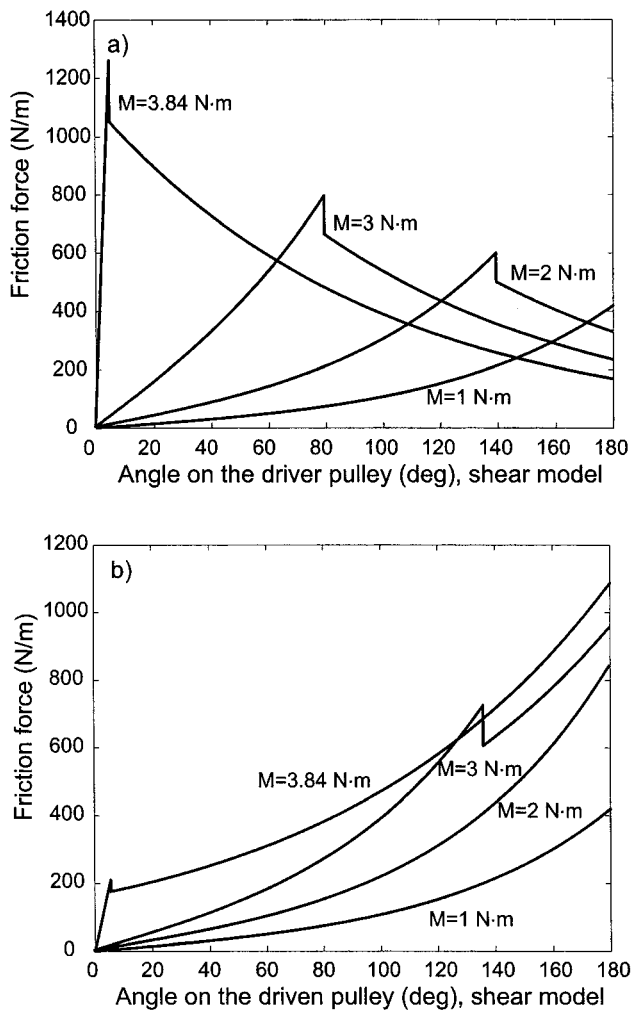


**Fig. 4** Variation of friction force per unit arclength of the shear model for the system specified in Table 1: (a) driver pulley and (b) driven pulley

which can be rewritten as  $V = (1 + F/EA)G/m_0$ , and  $EA$  is very large. The shape of the speed variation is similar to that of the belt tension.

For the shear model, initially there are only adhesion zones where the friction always increases from zero at the entry points. With increasing driving moment, the friction forces in the adhesion zones increase. This is realized mainly through the increased speed difference between belt and pulleys at the entry points (Fig. 8), whose effects are shown in equation (13). Once the maximum static friction is reached at the exit points, sliding zones emerge. Friction in these zones varies exponentially. Further increase of the driving moment leads to diminishment of the adhesion zones until the maximum transmissible moment is reached, as discussed later.

For the creep model, the adhesion zones decrease with the driving moment until the adhesion angle becomes zero; at this point, the drive reaches the maximum transmissible moment.

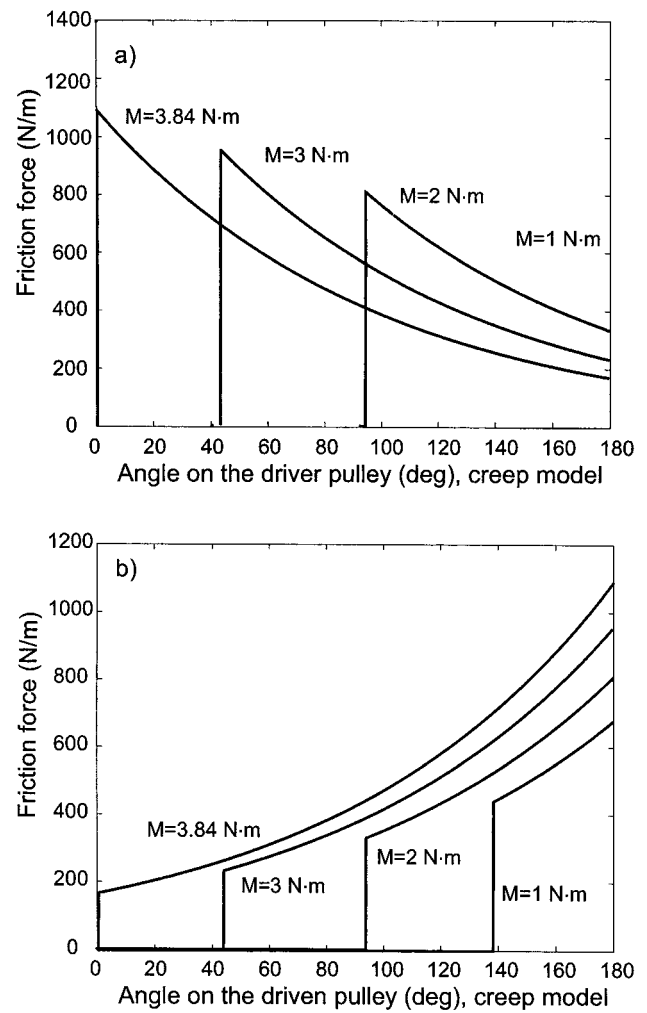


**Fig. 5** Variation of friction force per unit arclength of the creep model for the system specified in Table 1: (a) driver pulley and (b) driven pulley

For both models, the sliding zones, if they exist, always increase with the driving moment. The variations of the belt tension and speed in the sliding zones are similar (varying exponentially with the pulley angles) because the governing equations are the same. The differences between these two models lie mainly in the adhesion zone mechanics and the location of points dividing the contact arcs into adhesion and sliding zones.

Figure 8 shows the variation of free span and pulley speeds with the driving moment. Notice the different speed scales and the exploded region in Fig. 8(a), which matches the scale of Fig. 8(b). In the shear model (Fig. 8(a)), for power to be transmitted, the tight span speed is less than that of the driver pulley and the slack span speed is larger than that of the driven pulley (here the pulley speed refers to the linear speed of the pulley surface). From the constitutive law, the tight span speed is higher than that of the slack span because  $F_t > F_s$ .

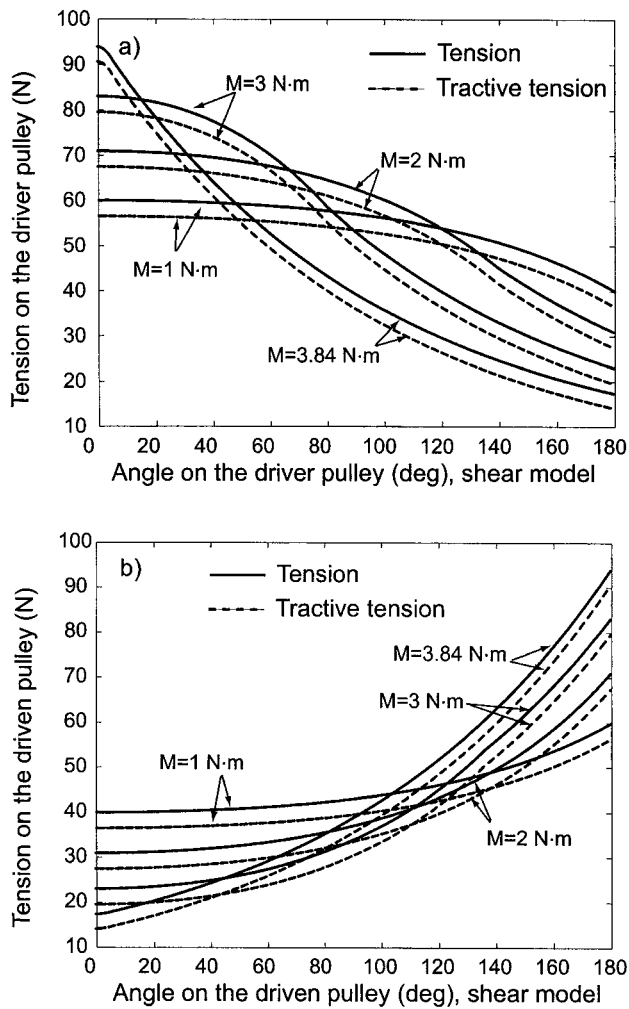


**Fig. 6** Variation of belt tension of the shear model for the system specified in Table 1: (a) driver pulley and (b) driven pulley

Thus, we have  $V_{\text{driver}} > V_{\text{tight}} > V_{\text{slack}} > V_{\text{driven}}$  (Fig. 8(a)). For the creep model, the tight (slack) span speed is always the same as that of the driver (driven) pulley [6–8], and the tight span speed is larger than that of the slack span (Fig. 8(b)).

The variations of free span tensions with driving moment are shown in Fig. 9. Figures 8 and 9, together with Fig. 3, show that the moment range in the shear model is larger than that in the creep model. This shows that the maximum transmissible moments calculated from these two models are different. For the creep model, as the driving moment increases, the adhesion angles  $\alpha_{1,2}$  on both pulleys decrease almost linearly (Fig. 3(b)). Once either or both of them reaches zero, no more moment can be transmitted without global slip, i.e. the maximum transmissible moment  $M_{\text{shear}}^{(\max)}$  is reached, as discussed in references [7, 8]. For the shear model, after the adhesion angles  $\alpha_{1,2}$  decrease close to zero, the transmitted moment can still be increased with little

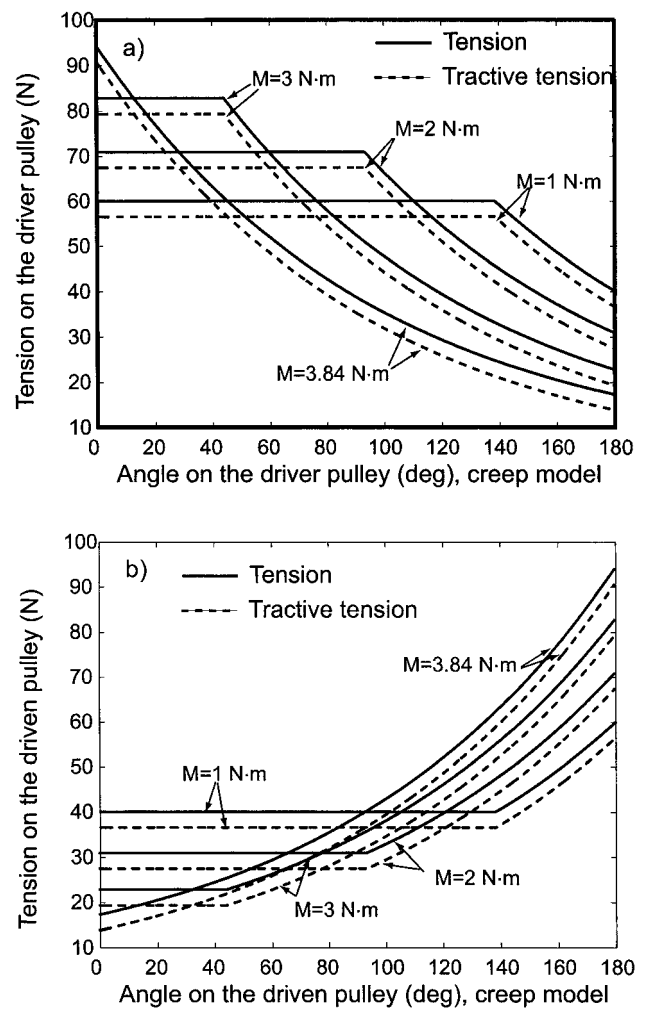


**Fig. 7** Variation of belt tension of the creep model for the system specified in Table 1: (a) driver pulley and (b) driven pulley

decrease in the adhesion angles (Fig. 3(a)). In this stage, the increased moment is achieved mainly from decrease of the belt and driven pulley speeds (Fig. 8(a)). Once the driven pulley speed, which is the lowest (because  $V_{\text{driver}} > V_{\text{tight}} > V_{\text{slack}} > V_{\text{driven}}$  as mentioned earlier), reaches zero, then the maximum transmissible moment  $M_{\text{shear}}^{(\max)}$  is reached and no more moment can be carried. In this stage, the speeds of the belt and the driven pulley decrease dramatically with the driving moment (Fig. 8(a)), and the belt tractive tensions  $T = F - GV$  approach the normal tensions quickly (Fig. 9(a)), while the adhesion/sliding angles vary only slightly (Fig. 3(a)). It is the difference between the tight (slack) span speed and the driver (driven) pulley speed that enables more moment to be transmitted in the shear model. At the point of the maximum transmissible moment, the belt speed is very small. The adhesion angles are non-zero, although very small.

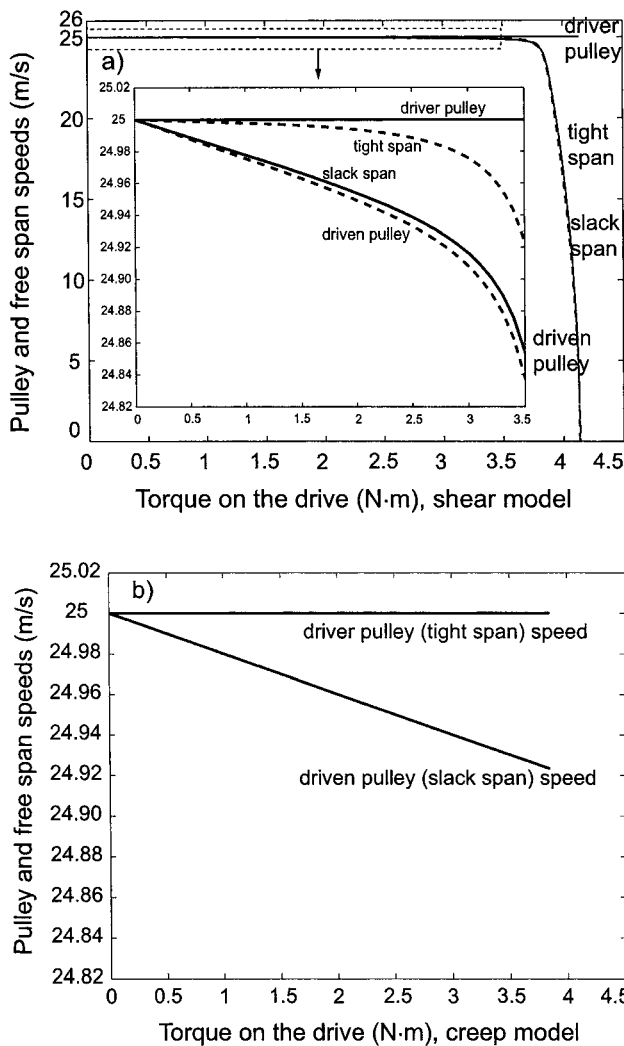


**Fig. 8** Variation of free span and pulley speeds with the driving moment for the system specified in Table 1: (a) shear model and (b) creep model

The variation of mass flow rate  $G$  and power efficiency  $\eta = (M_2\omega_2)/(M_1\omega_1)$  with the driving moment is shown in Figs 10 and 11. The differences between these two models only become pronounced when  $M > M_{\text{creep}}^{\text{max}}$ . As the shear model admits larger moments than the creep model, operation at these high moments is inefficient.

The creep model is more applicable for belts with uniform cross-section such as metal belts in band saws or in some modern continuously variable transmission, and this model has been experimentally confirmed (fig. 5.4 in reference [1]). The shear model is more applicable for modern belts with grid layers, the experimental support can be found in chapter 41 of reference [1]. Although the variation of the tension, speed, and friction in the belt-pulley contact arcs is dramatically different in these two models (as indicated in Figs 3 to 7), differences in

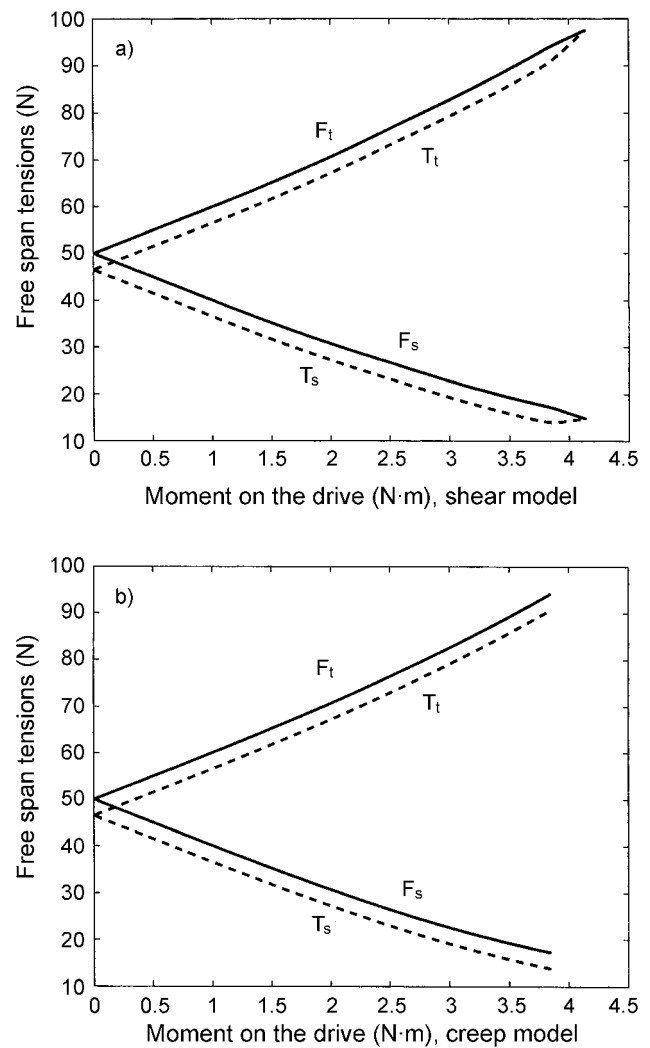


**Fig. 9** Variation of free span tension with the driving moment for the system specified in Table 1: (a) shear model and (b) creep model

the overall system performance in terms of the free span tension speed, maximum transmissible moment, and power efficiency are small for most normal operating conditions. From practical perspective, it is fine to use either of these two models when dealing with flat belts in the most industrial applications.

## 5 CONCLUSIONS

Steady motion analysis based on the shear microslip model is applied to a two-pulley belt drive. The belt is modelled as an axially moving string with belt inertia fully considered. A three-loop iteration method is developed to find the solution to arbitrary accuracy. Comparison with the well-known creep theory is conducted. Mathematically, the shear model is

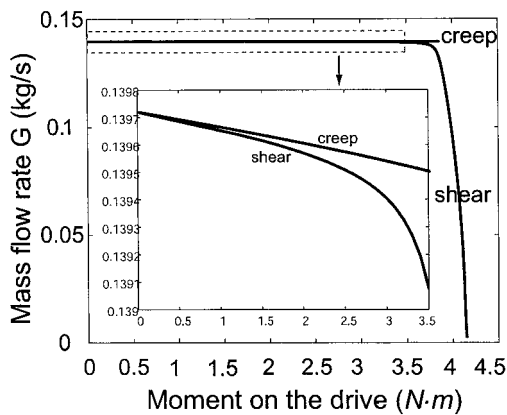


**Fig. 10** Variation of mass flow rate  $G$  with the driving moment for the system specified in Table 1

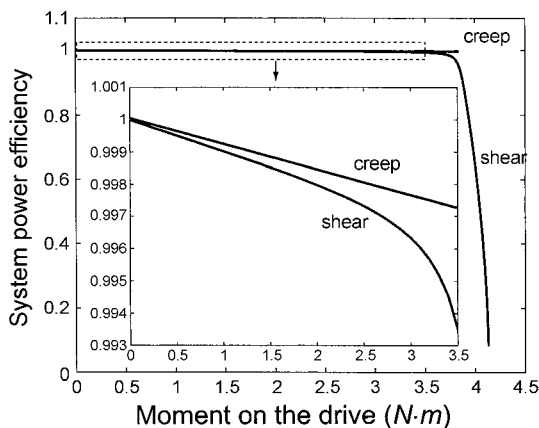


**Fig. 11** Variation of system power efficiency with the driving moment for the system specified in Table 1

more complicated than the creep model. It allows for speed differences between the pulleys and the free spans, requiring additional effort to solve (e.g. the two inner loops).

The main conclusions are as follows.

1. The distributions of the belt tension, speed, and friction in the belt–pulley contact arcs are markedly different in qualitative and quantitative terms for the shear and creep models. The differences in overall system performance between these two models, including belt tension variation ranges and system power efficiencies, are small for most of the driving moment range  $0 < M < M_{\text{creep}}^{(\max)}$ .
2. Different from the creep model, the shear model allows the possibility that only adhesion zones exist on both the driver and the driven pulleys to

transmit power when the driving moment is small.

3. For the creep model, the maximum transmissible moment is reached when one of the adhesion angles decreases to zero, whereas for the shear model, the maximum transmissible moment is reached when the driven pulley speed is zero, even though there is a very small adhesion zone in this case.
4. The maximum transmissible moment for the shear model is larger than that for the creep model. This is realized through dramatic decreases of the belt and the driven pulley speeds.

## ACKNOWLEDGEMENT

The authors thank Mark IV Automotive/Dayco Corporation and the National Science Foundation for support of this research.

## REFERENCES

- 1 **Gerbert, G.** *Traction belt mechanics*, 1999 (Chalmers University of Technology, Sweden).
- 2 **Grashof, F.** *Teoretische Maschinenlehre*, Band 2, 1883 (Leopold Voss, Hamburg).
- 3 **Euler, M. L.** Remarques Sur L'effect Du Frottement Dans L'equilibre. *Mem. Acad. Sci.*, 1762, 265–278.
- 4 **Fawcett, J. N.** Chain and belt drives—a review. *Shock Vib. Digest*, 1981, **13**(5), 5–12.
- 5 **Johnson, K. L.** *Contact mechanics*, 1985 (Cambridge University Press, New York).
- 6 **Bechtel, S. E., Vohra, S., Jacob, K. I., and Charlson, C. D.** The stretching and slipping of belts and fibers on pulleys. *J. Appl. Mech.*, 2000, **67**, 197–206.
- 7 **Rubin, M. B.** An exact solution for steady motion of an extensible belt in multipulley belt drive systems. *J. Mech. Design*, 2000, **122**, 311–316.
- 8 **Kong, L. and Parker, R. G.** Steady mechanics of belt–pulley systems. *J. Appl. Mech.*, 2005, **72**(1), 25–34.
- 9 **Kong, L. and Parker, R. G.** Mechanics of serpentine belt drives with tensioner assemblies and belt bending stiffness. *J. Mech. Design*, 2005, **127**, 957–966.
- 10 **Gerbert, G.** Belt slip—a unified approach. *J. Mech. Design*, 1996, **118**, 432–438.
- 11 **Kong, L. and Parker, R. G.** Mechanics and sliding friction in belt drives with pulley grooves. *J. Mech. Design*, in press.
- 12 **Firbank, T. C.** Mechanics of belt drives. *Int. J. Mech. Sci.*, 1970, **12**, 1053–1063.
- 13 **Menq, C. H., Bielak, J., and Griffin, J. H.** The influence of microslip on vibratory response. Part I: a new microslip model. *J. Sound Vib.*, 1986, **107**(2), 279–293.
- 14 **Leamy, M. J.** On a perturbation method for the analysis of unsteady belt-drive operation. *J. Appl. Mech.*, 2005, **72**, 570–580.